Inorg. Chem. **2008**, *47*, 11324−11333

Halide Ligands—More Than Just σ-Donors? A Structural and Spectroscopic Study of Homologous Organonickel Complexes

Axel Klein,[†,*] André Kaiser,[†] Wolfram Wielandt,[‡,§] Ferdinand Belaj,[‡] Eric Wendel,[||] Helmut Bertagnolli,[||] and Stanislav Záliš[⊥]

Universität zu Köln, Department für Chemie, Bereich Anorganische Chemie, Greinstraße 6, D-50939 Köln, Germany, Karl-Franzens-Universität Graz, Institut für Chemie, Schubertstraße 1, A-8010 Graz, Austria, Universität Stuttgart, Institut für Physikalische Chemie, Pfaffenwaldring 55, D-70569, Stuttgart, Germany, and J. Heyrovský Institute of Physical Chemistry, Academy of Sciences of the Czech Republic, Dolejškova 3, CZ-18 000 Prague 8, Czech Republic

Received April 24, 2008

The isoleptic organonickel complexes [(bpy)Ni(Mes)X] (bpy = 2,2′-bipyridine; Mes = 2,4,6-trimethylphenyl; X = F, Cl, Br, or I, and for comparison X = OMe and SCN) have been investigated by multiple spectroscopic means. Their structures have been determined in part by single-crystal X-ray diffraction, the full series by extended X-ray absorption fine structure. The long-wavelength charge transfer absorptions (mainly metal-to-ligand charge transfer) obtain contributions from the mesityl coligand but are almost invariable upon variation of X. UV−vis spectroscopy allowed investigation of the solvolysis reaction [(bpy)Ni(Mes)X] + Solv ⇄ [(bpy)Ni(Mes)(Solv)]$^+$ + X$^-$, which occurs very fast for X = I (k = 0.176(4) M^{-1} s^{-1}) or Br but very slow for X = Cl (k = 5.18(5) × 10^{-5} M^{-1} cm^{-1}) or F. Quantum chemical (density functional theory) calculations on the geometry, electronic states, and electronic transitions (time-dependent density functional theory) are very helpful for detailed insight into the role the X coligands play in these complexes. The combination of methods reveals rather strong, highly covalent Ni−X bonds for all halide coligands but marginal π-donation.

Introduction

Organometallic nickel complexes with α-diimine ligands like 2,2′-bipyridine (bpy), 1,10-phenanthroline, or diazabutadienes have gained enormous interest in the past decade. This is mainly due to a number of important catalytic processes like olefin oligo- or polymerization, olefin/CO copolymerization,[1] and various (electro)catalytic C−C coupling reactions.[2−9] Paralleling their use in catalysis, fundamental studies on structures and

* Author to whom correspondence should be addressed. E-mail: axel.klein@uni-koeln.de.
† Universität zu Köln.
‡ Karl-Franzens-Universität Graz.
§ Present address: EPCOS OHG, Deutschlandsberg, Austria.
|| Universität Stuttgart.
⊥ Academy of Sciences of the Czech Republic.

(1) (a) Cornils, B.; Herrmann, W. A. *Applied Homogeneous Catalysis with Organometallic Compounds*, 2nd ed.; Wiley/VCH: Weinheim, Germany; 2002. (b) Ittel, S. D.; Johnson, L. K.; Brookhart, M. *Chem. Rev.* **2000**, *100*, 1169–1203. (c) Michalak, A.; Ziegler, T. *Organometallics* **2001**, *20*, 1521–1532. (d) Mecking, S. *Angew. Chem., Int. Ed. Engl.* **2001**, *40*, 534–540. (e) Gibson, V. C.; Spitzmesser, S. K. *Chem. Rev.* **2003**, *103*, 283–315. (f) Yakhvarov, D. G.; Tazeev, D. I.; Sinyashin, O. G.; Giambastiani, G.; Bianchini, C.; Segarra, A. M.; Lönnecke, P.; Hey-Hawkins, E. *Polyhedron* **2006**, *25*, 1607–1612. (g) Meinhard, D.; Reuter, P.; Rieger, B. *Organometallics* **2007**, *26*, 751–754. (h) Chen, Q.; Yu, J.; Huang, J. *Organometallics* **2007**, *26*, 617–625.

(2) (a) Moinet, C.; Hurvois, J.-P.; Jutand, A. *Adv. Org. Synth.* **2005**, *1*, 403–453. (b) Amatore, C.; Jutand, A.; Périchon, J.; Rollin, Y. *Monatsh. Chem.* **2000**, *131*, 1293–1304.

(3) (a) Nédélec, J.-Y.; Périchon, J.; Troupel, M. *Top. Curr. Chem.* **1997**, *185*, 141–173. (b) Durandetti, M.; Périchon, J. *Synthesis* **2004**, 3079–3083. (c) Raynal, F.; Barhdadi, R.; Périchon, J.; Savall, A.; Troupel, M. *Adv. Synth. Catal.* **2002**, *344*, 45–49.

(4) (a) Budnikova, Y. H. *Russ. Chem. Rev.* **2002**, *71*, 111–139. (b) Yakhvarov, D. G.; Budnikova, Y. H.; Sinyashin, O. G. *Russ. J. Electrochem.* **2003**, *39*, 1261–1269. (c) Yakhvarov, D. G.; Budnikova, Y. H.; Sinyashin, O. G. *Mendeleev Commun.* **2002**, 175–176. (d) Budnikova, Y. H.; Périchon, J.; Yakhvarov, D. G.; Kargin, Y. M.; Sinyashin, O. G. *J. Organomet. Chem.* **2001**, *630*, 185–192. (e) Budnikova, Y. H.; Kargin, Y. M.; Nédélec, J.-Y.; Périchon, J. *J. Organomet. Chem.* **1999**, *575*, 63–66.

(5) Klein, A.; Budnikova, Y. H.; Sinyashin, O. G. *J. Organomet. Chem.* **2007**, *692*, 3156–3167.

(6) (a) Corbet, J.-P.; Mignani, G. *Chem. Rev.* **2006**, *106*, 2651–2710. (b) Anctil, E. J.; Snieckus, G. V. In *Metal-Catalyzed Cross-Coupling Reactions*, 2nd ed.; De Meijere, A., Dieterich, F., Eds.; Wiley: Weinheim, Germany, 2004; Vol. *76*, pp 1−813.

(7) Tamao, K. *J. Organomet. Chem.* **2002**, *653*, 23–26.

(8) (a) Yamamoto, T. *Synlett* **2003**, *4*, 425–450. (b) Osakada, K.; Yamamoto, T. *Coord. Chem. Rev.* **2000**, *198*, 379–399. (c) Yamamoto, T.; Wakabayashi, S.; Osakada, K. *J. Organomet. Chem.* **1992**, *428*, 223–237.

10.1021/ic8007365 CCC: $40.75
Published on Web 10/29/2008

electronic properties of organonickel complexes with α-diimines have been carried out.[9−11] We have contributed to this with the investigation of a number of organonickel complexes [(N^N)Ni(Mes)Br] (N^N = α-diimine ligands, Mes = mesityl = 2,4,6-trimethylphenyl) with various diimine ligands. Their structures and reactivity toward ligand exchange reactions have been studied using X-ray diffraction and absorption spectroscopy;[12,13] their photophysics and photochemistry were explored by a combination of multiple spectroscopy and quantum chemical calculations,[12,14] and finally, their redox chemistry was investigated,[15] with respect to the application of such systems in electrocatalytical C−C coupling reactions.[5]

Summarizing all of these studies, a considerable contribution of the bromide coligand can be stated. (i) In the presence of strongly donating solvents like nitriles, N,N-dimethylformamide (DMF), or dimethylsulfoxide (DMSO), ligand exchange reactions occur, releasing the bromide ligand (eq 1), whereas in acetone, ethers, or chlorinated solvents, the complexes were stable.[13]

$$[(L)_2Ni(Mes)Br] + L' \rightleftharpoons [(L)_2Ni(Mes)L]^+ + Br^- \quad (1)$$

L = PPh_3 or bpy/2; L′ = strong donation solvents

(ii) A thorough study of the photophysical properties of the complex [(bpy)Ni(Mes)Br] revealed an appreciable contribution of the Br coligand to the electronic transitions, as inferred from quantum chemical calculations of the ground state, excited states, and electronic transitions by time-dependent density functional theory (TD DFT).[14] (iii) After $1e^-$ reduction, the complexes [(N^N)Ni(Mes)Br] (N^N = various α-diimine ligands) undergo a very fast cleavage of the bromide coligand (eq 2).[15]

$$[(N^N)Ni(Mes)Br] \overset{+e^-}{\rightleftharpoons} [(N^N)Ni(Mes)Br]^{\bullet -} \rightleftharpoons [(N^N)Ni(Mes)]^{\bullet} + Br^- \quad (2)$$

As a consequence of these studies, we have prepared the four isoleptic complexes [(bpy)Ni(Mes)X] (bpy = 2,2′-bipyridine; Mes = 2,4,6-trimethylphenyl; X = F, Cl, Br, or I) and investigated them by multiple spectroscopy and electrochemistry to probe for the role of the coligand X to both reactivity and electronic states.

There are two main issues in the metal−ligand interaction in coordination chemistry. One is regarding the character of the M−L σ bond (covalent vs ionic); the other is addressing the question of whether there are further interactions between the metal and ligand beyond the M−L σ bond, such as π bonds (π-accepting, π-donating). Both aspects will be addressed in this study, to which we have added, for the sake of comparison, also the complexes with the pseudohalides X = OMe and SCN.

Experimental Section

Materials. Commercially available PPh_3 (Aldrich), $NiCl_2$, $NiBr_2$ (Chempur), and MesBr (Acros) were used without further purification.

Instrumentation. ^1H NMR spectra were recorded using Bruker Avance 300 (^1H, 300.13 MHz; ^{13}C, 75.47 MHz; ^{19}F, 282.35 MHz) or Bruker Avance 400 spectrometers (^1H, 400.13 MHz; ^{13}C, 100.61 MHz; ^{19}F, 376.50 MHz), the latter using a triple resonance ^1H,^{19}F,BB inverse probe head. The unambiguous assignment of the ^1H and ^{13}C resonances was obtained from ^1H nuclear Overhauser effect spectrometry; ^1H correlation spectroscopy; and gradient-selected ^1H and ^{13}C heteronuclear single quantum coherence and heteronuclear multiple-bond correlation experiments. All 2D NMR experiments were performed using standard pulse sequences from the Bruker pulse program library. Chemical shifts were relative to tetramethylsilane and CCl_3F. UV−vis absorption spectra were recorded with Varian Cary 05E or Cary 50 scan spectrophotometers. Kinetic measurements were performed in an acetone solution (2 mL acetone) using a Cary 50 scan spectrophotometer. After the admixture of 0.5 mL of acetonitrile, the decay of the long-wavelength absorption band at about 460 nm was recorded and fitted assuming a first-order mechanism (monoexponential decay). Elemental analyses were obtained using a HEKAtech CHNS EuroEA 3000 analyzer. IR and Raman spectra of the complexes dispersed in KNO_3 pellets were recorded with a Bruker IFS/66v/S spectrometer equipped with a FRA106/S module for Raman measurements, using a Nd:YAG laser (λ = 1064 nm) as the excitation source. Electrochemical measurements were carried out at a 100 mV/s scan rate in 0.1 M Bu_4NPF_6 solutions using a three-electrode configuration (glassy carbon electrode, Pt counter electrode, Ag/AgCl reference) and a Metrohm Autolab PGSTAT30 potentiostat and function generator. The ferrocene/ferrocenium couple served as the internal reference.

Crystal Structure Analysis for [(bpy)Ni(Mes)Cl] and [(bpy)Ni(Mes)I]. Crystals of both compounds were obtained from concentrated solutions in toluene. The measurements for [(bpy)Ni(Mes)Cl] were performed at 293(2) K using IPDS II (STOE and Cie.), and the data for [(bpy)Ni(Mes)I] were obtained using a STOE four-circle diffractometer at 100(2) K, both using graphite-monochromatized Mo Kα radiation. The structures were solved by direct methods (*SHELXS 97*)[16] and refined by full-matrix least-squares techniques against F^2 (*SHELXL 97*).[17] The non-hydrogen atoms were refined with anisotropic displacement parameters without any constraints. The hydrogen atoms were included by using appropriate riding models. Details of the crystal structure solutions and refinements were summarized in Table 1. Full structural information for [(bpy)Ni(Mes)Cl] and [(bpy)Ni(Mes)I] has been deposited with the Cambridge Crystallographic Data Centre, No. CCDC 659485 (X = Cl) and No. CCDC 659486 (X = I). Copies of the data can be obtained, free of charge, upon application to CCDC, 12 Union Road, Cambridge CB2 1EZ, U.K. (fax: +44−1223 336033 or e-mail: deposit@ccdc.cam.ac.uk).

(9) (a) Yamamoto, T.; Abla, M.; Murakami, Y. *Bull. Chem. Soc. Jpn.* **2002**, *75*, 1997–2009. (b) Yamamoto, T.; Abla, M. *J. Organomet. Chem.* **1997**, *535*, 209–211. (c) Uchino, M.; Asagi, K.; Ymamoto, A.; Ikeda, S. *J. Organomet. Chem.* **1975**, *84*, 93–103. (d) Yamamoto, T.; Yamamoto, A.; Ikeda, S. *J. Am. Chem. Soc.* **1971**, *93*, 3350–3359.

(10) (a) Tucci, G. C.; Holm, R. H. *J. Am. Chem. Soc.* **1995**, *117*, 6489–6496. (b) Arcas, A.; Royo, P. *Inorg. Chim. Acta* **1978**, *31*, 97–99. (c) Arcas, A.; Royo, P. *Inorg. Chim. Acta* **1978**, *30*, 205–207.

(11) De Souza, R. F.; Simon, L. C.; Alves, M. C. *J. Catal.* **2003**, *214* (1), 165–168.

(12) Klein, A. *Z. Anorg. Allg. Chem.* **2001**, *627*, 645–650.

(13) Feth, M. P.; Klein, A.; Bertagnolli, H. *Eur. J. Inorg. Chem.* **2003**, *83*, 9–852.

(14) Feth, M. P.; Klein, A.; Bertagnolli, H.; Záliš, S. *Eur. J. Inorg. Chem.* **2004**, 2784–2796.

(15) Klein, A.; Kaiser, A.; Sarkar, B.; Wanner, M.; Fiedler, J. *Eur. J. Inorg. Chem.* **2007**, *96*, 5–976.

(16) Sheldrick, G. M. *SHELXS 97*; University of Göttingen: Göttingen, Germany, 1997.

(17) Sheldrick, G. M. *SHELXL 97*; University of Göttingen: Göttingen, Germany, 1997.

Table 1. Selected Crystallographic Data for [(bpy)Ni(Mes)X] (X = Cl or I)

formula/fw	$C_{19}H_{19}ClN_2Ni/369.52$	$C_{19}H_{19}IN_2Ni/460.95$
cryst syst/space group	monoclinic/$P2_1/n$	monoclinic/$P2_1/c$
cell a	11.323(2) Å	16.744(6) Å
b	9.7350(19) Å	12.624(4) Å
c	16.524(3) Å	17.824(6) Å
β	102.83(3)°	108.98(3)°
vol (Å^3)/Z	1775.8(6)/4	3563(2)/8
calcd density (Mg/m^3)/F(000)	1.382/768	1.719/1824
μ (mm^{-1})/temp (K)	1.243/293(2)	2.822/100(2)
Θ range for data collection	2.44 to 28.18°	2.57 to 26.00°
index ranges	$-15 \le h \le 14$, $-12 \le k \le 12$, $-21 \le l \le 21$	$-20 \le h \le 19$, $-1 \le k \le 15$, $-1 \le l \le 21$
reflns collected/unique	4041/2566	8508/6978
R(int)/completeness to Θ_{max}	0.075/93.2%	0.0289/99.8%
data/params/restraints	4041/211/0	6978/427/0
goodness-of-fit on F^2	0.904	1.088
final R indices [I > 2σ(I)]	$R_1 = 0.0401$, $wR_2 = 0.0904$	$R_1 = 0.0456$, $wR_2 = 0.1040$
R indices (all data)	$R_1 = 0.0726$, $wR_2 = 0.1019$	$R_1 = 0.0603$, $wR_2 = 0.1122$
largest difference peak and hole (e/Å^3)	0.508 and −0.382	1.108 and −1.255

Table 2. ^{1}H NMR Data of [(bpy)Ni(Mes)X] in Acetone-d^6 (Numbering as in Scheme 1)

	δ (in ppm)						
compound	6, 6′	3, 3′	4, 4′	5, 5′	m-H	o-CH$_3$	p-CH$_3$
bpy (free ligand)	8.66	8.47	7.91	7.40			
X = F	9.46, 7.22	8.36, 8.33		7.73, 7.34	6.46	3.06	2.19
X = Cl	9.43, 7.22	8.37, 8.34	8.22, 8.17	7.73, 7.36	6.47	3.06	2.20
X = Br	9.43, 7.20	8.36, 8.33	8.21, 8.15	7.71, 7.35	6.45	3.05	2.19
X = I	9.70, 7.41	8.41, 8.40	8.20, 8.19	7.69, 7.03	6.48	3.00	2.20
X = OMe	8.92, 7.56	8.34, 8.22	8.20, 8.06	7.72, 7.23	6.58	3.10	2.20
X = SCN	8.60, 7.26	8.44, 8.37	8.32, 8.17	7.88, 7.39	6.52	3.04	2.20

Scheme 1. Numbering of the Protons in the Complexes [(bpy)Ni(Mes)X]

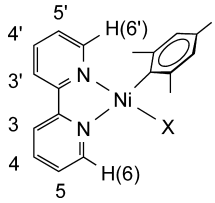

X-Ray Spectroscopy. The X-ray absorption near edge structure (XANES) and extended X-ray absorption fine structure (EXAFS) measurements were performed at the XAS beamline, ANKA, Karlsruhe. For the measurements at the Ni K edge (8333 eV), a Si(111) double-crystal monochromator was used. The tilt of the second monochromator crystal was set to 40% harmonic rejection. The spectra were collected under ambient conditions at 21 °C in transmission mode with ion chambers. All ion chambers were filled with nitrogen. Energy calibration was performed with nickel foil. The solid samples were embedded in a cellulose matrix and pressed to pellets. Data evaluation started with the removal of background absorption from the experimental spectrum by subtraction of a Victoreen-type polynomial, which was fitted to the pre-edge region of the spectrum. This step and also the following normalization of the spectrum were performed with the program WinXAS.[18] After the normalization, the program AUTOBK[19] was used to remove the postedge background and to isolate the EXAFS function $\chi(k)$. A curve-fitting analysis of the EXAFS function, weighted with k^3, was performed according to the curved wave formalism of the program EXCURV98 with XALPHA phase and amplitude functions.[20] The mean free path of the scattered electrons was calculated from the imaginary part of the potential (VPI set to −4.00); the amplitude reduction factor (AFAC) was fixed at 0.8, and an overall energy shift (E_f) was introduced to give a best fit to the data.

Computational Details. Ground-state electronic structure calculations on complexes [(bpy)Ni(Mes)X] (X = F, Cl, Br, I) have been done on the basis of DFT methods using the Gaussian 03[21] and ADF2006.01[22] program packages. The lowest excited states of the closed shell complexes were calculated by the TD DFT method.

Within the ADF program, Slater-type orbital basis sets of triple-ζ quality with two polarization functions for the Ni atom and with one polarization function for the remaining atoms were employed; methyl groups on the Mes coligands were described by basis sets of double-ζ quality with polarization functions. The inner shells were represented by a frozen core approximation (1s for C, N, and F; 1s-2p for Cl; 1s-3p for Br; and 1s-3p for Ni and 1s-4p for I were kept frozen). Within ADF, the functional including Becke's gradient correction to the local exchange expression in conjunction

(18) Ressler, T. *J. Synch. Radiat.* **1998**, *5*, 118–122.
(19) Newville, M.; Livins, P.; Yakoby, Y.; Rehr, J. J.; Stern, E. A. *Phys. Rev. B* **1993**, *47*, 14126–14131.
(20) Gurman, S. J.; Binsted, N.; Ross, I. *J. Phys. C* **1986**, *19*, 1845–1861.
(21) Frisch, M. J.; Trucks, G. W.; Schlegel, H. B.; Scuseria, G. E.; Robb, M. A.; Cheeseman, J. R.; Montgomery, J. A., Jr.; Vreven, T.; Kudin, K. N.; Burant, J. C.; Millam, J. M.; Iyengar, S. S.; Tomasi, J.; Barone, V.; Mennucci, B.; Cossi, M.; Scalmani, G.; Rega, N.; Petersson, G. A.; Nakatsuji, H.; Hada, M.; Ehara, M.; Toyota, K.; Fukuda, R.; Hasegawa, J.; Ishida, M.; Nakajima, T.; Honda, Y.; Kitao, O.; Nakai, H.; Klene, M.; Li, X.; Knox, J. E.; Hratchian, H. P.; Cross, J. B.; Bakken, V.; Adamo, C.; Jaramillo, J.; Gomperts, R.; Stratmann, R. E.; Yazyev, O.; Austin, A. J.; Cammi, R.; Pomelli, C.; Ochterski, J. W.; Ayala, P. Y.; Morokuma, K.; Voth, G. A.; Salvador, P.; Dannenberg, J. J.; Zakrzewski, V. G.; Dapprich, S.; Daniels, A. D.; Strain, M. C.; Farkas, O.; Malick, D. K.; Rabuck, A. D.; Raghavachari, K.; Foresman, J. B.; Ortiz, J. V.; Cui, Q.; Baboul, A. G.; Clifford, S.; Cioslowski, J.; Stefanov, B. B.; Liu, G.; Liashenko, A.; Piskorz, P.; Komaromi, I.; Martin, R. L.; Fox, D. J.; Keith, T.; Al-Laham, M. A.; Peng, C. Y.; Nanayakkara, A.; Challacombe, M.; Gill, P. M. W.; Johnson, B.; Chen, W.; Wong, M. W.; Gonzalez, C.; Pople, J. A. *Gaussian 03*, revision C.02; Gaussian, Inc.: Wallingford, CT, 2004.
(22) ADF 2006.1: (a) te Velde, G.; Bickelhaupt, F. M.; van Gisbergen, S. J. A.; Fonseca Guerra, C.; Baerends, E. J.; Snijders, J. G.; Ziegler, T. *J. Comput. Chem.* **2001**, *22*, 931–967. ADF 2005.01: (b) *SCM*; Vrije Universiteit: Amsterdam, The Netherlands. http://www.scm.com (accessed Oct 10, 2008).

with Perdew's gradient correction to local density approximation with VWN parametrization of electron gas data was used (ADF/BP).[23,24] The scalar relativistic zero-order regular approximation was used in ADF. Within Gaussian 03, polarized valence double-ζ basis sets[25] were used for C, N, H and X atoms and for Ni.[26] The hybrid Becke's three-parameter functional with the Lee, Yang, and Parr correlation functional (B3LYP)[23] was used in Gaussian 03 calculations (G03/B3LYP). The conductor-like polarizable continuum model (CPCM)[27] was used for modeling of the solvent influence in TD DFT calculations. The calculations on complexes were performed without any symmetry constraints. Spectral calculations were done at optimized geometries using an identical method.

Preparation of the Precursor Complexes *trans*-[$(PPh_3)_2$-Ni(Mes)X]. The precursor complexes *trans*-[$(PPh_3)_2$Ni(Mes)X] (X = Cl or Br) were prepared from anhydrous NiX_2, PPh_3, and corresponding Grignard reagents MesMgX, as recently described for *trans*-[$(PPh_3)_2$Ni(Mes)Br].[12] *trans*-[$(PPh_3)_2$Ni(Mes)Cl] was obtained as a yellow powder, yield 17%. Anal. calcd for $C_{45}H_{41}ClNiP_2$ (737.92): C, 73.25; H, 5.60. Found: C, 73.31; H, 5.65%. ^{1}H NMR (CD_2Cl_2): δ 7.47 (m, 12H, *o*-Ph); 7.33 (m, 6H, *p*-Ph); 7.22 (m, 12H, *m*-Ph); 5.79 (s, 2H, HMes); 2.34 (s, 6H, *o*-CH_3); 1.89 (s, 3H, *p*-CH_3). ^{31}P NMR (CD_2Cl_2): δ 18.67. ^{13}C NMR (CD_2Cl_2): δ 142.1 (Mes1), 142.3 (Mes2), 135.2 (Ph2), 133.2 (Mes4), 132.5 (Ph1), 130.0 (Ph4), 128.0 (Ph3), 127.5 (Mes3), 26.1 (*o*-CH_3), 19.9 (*p*-CH_3).

Preparation of the Complexes [(bpy)Ni(Mes)X] (X = F, Cl, Br, I). The complexes with X = Cl or Br were synthesized by stirring the precursor complexes *trans*-[$(PPh_3)_2$Ni(Mes)X] (typically 1.38 g, 1.87 mmol for X = Cl) with bpy (310 mg, 1.964 mmol) in diethyl ether (100 mL) at ambient temperature for 24 h. The resulting dark red suspensions were filtered; the collected precipitate was rinsed with *n*-pentane (50 mL) and dried under a vacuum. The yield for X = Cl was 0.57 g, 1.543 mmol, 83%. Anal. calcd for $C_{19}H_{19}ClN_2Ni$ (369.52): C, 61.76; H, 5.18; N, 7.58. Found: C, 61.81; H, 5.25; N, 7.61%. ^{1}H NMR (acetone-d^6): See Table 2. [(bpy)Ni(Mes)Br] was obtained under the same conditions at 95% yield. Anal. calcd for $C_{19}H_{19}BrN_2Ni$ (431.98): C, 55.12; H, 4.63; N, 6.77. Found: C, 55.33; H, 4.65; N, 6.72%. ^{1}H NMR (acetone-d^6): See Table 2.

Preparation of [(bpy)Ni(Mes)F]. To a solution of [(bpy)Ni-(Mes)Br] (0.99 g, 2.391 mmol) in 1,2-dichloroethane (30 mL) was added TlF (0.70 g, 3.133 mmol), and the resulting solution was stirred at 60 °C for 18 h. The mixture was concentrated under a vacuum to 10 mL, filtered, and treated with *n*-pentane (60 mL) to precipitate the product. Yield: 310 mg, 0.878 mmol, 37%. Anal. calcd for $C_{19}H_{19}FN_2Ni$ (353.08): C, 64.63; H, 5.42; N, 7.93. Found: C, 64.70; H, 5.45; N, 7.94%. ^{1}H NMR (acetone-d^6): See Table 2. ^{19}F NMR (acetone-d^6): δ −407.1 (s).

Preparation of [(bpy)Ni(Mes)I]. A solution of [(bpy)Ni(Mes)Cl] (0.57 g, 1.543 mmol) and dry NaI (1.16 g, 7.713 mmol) in dry acetone (20 mL) was refluxed for 20 h. All volatile parts were removed under a vacuum, and the solid residue was extracted with 1,2-dichloroethane. Upon the addition of *n*-pentane (70 mL), a dark red precipitate formed that was filtered and dried under a vacuum. Yield: 0.43 g, 0.926 mmol, 60%. Anal. calcd for $C_{19}H_{19}IN_2Ni$ (460.95): C, 49.50; H, 4.15; N, 6.08. Found: C, 49.81; H, 4.25; N, 6.11%. ^{1}H NMR (acetone-d^6): See Table 2.

Preparation of [(bpy)Ni(Mes)(OMe)]. A total 100 mg of solid sodium (4.35 mmol)] was dissolved in 50 mL of terahydrofuran (THF) and 10 mL of methanol. To this solution was added 400 mg (0.966 mmol) of [(bpy)Ni(Mes)Br], the resulting solution was stirred for 12 h. The reaction mixture was evaporated to dryness, and the dark residue was extracted with 5 × 20 mL of dichloromethane. After evaporation of the solvent, the resulting material was twice recrystallized from dichloromethane/*n*-heptane (1:1) to yield 290 mg (0.79 mmol, 82%) of violet microcrystalline material. Anal. calcd for $C_{20}H_{22}O_1N_2Ni$ (365.12): C, 65.79; H, 6.07; N, 7.67. Found: C, 65.72; H, 5.99; N, 7.71%. ^{1}H NMR (acetone-d^6): See Table 2; for the O*CH*$_3$ protons, a signal was found at 3.29 ppm (s, 3H). ^{13}C NMR (acetone-d^6): δ 156.5 (bpy2), 153.5 (bpy2′), 153.1 (bpy6), 151.7 (bpy6′), 148.6 (Mes1), 143.5 (Mes2), 139.8 (bpy4), 137.9 (bpy4′), 133 (Mes4), 127.4 (bpy3), 126.7 (bpy3′), 126.2 (Mes3), 122.6 (bpy5), 121.3 (bpy5′), 49.6 (O*C*H$_3$), 25.8 (*o*-CH_3), 20.9 (*p*-CH_3). UV−vis (acetone): 468, 540sh nm.

Preparation of [(bpy)Ni(Mes)(SCN)]. To a total of 158 mg (0.38 mmol) of [(bpy)Ni(Mes)Br] dissolved in 50 mL of THF was added 131 mg (0.38 mmol) of $AgSbF_6$, and the resulting solution was stirred in the dark for 90 min. The colorless solution obtained from careful filtration was added to 37 mg (0.38 mmol) of KSCN suspended in 10 mL of THF. The mixture was heated under reflux for 3 h. The resulting orange solution was separated from some colorless precipitate and evaporated to dryness. Recrystallization from dichloromethane gave 121 mg (0.308 mmol, 81%) of orange-red material. Anal. calcd for $C_{20}H_{19}S_1N_3Ni$ (392.16): C, 61.26; H, 4.88; N, 10.72. Found: C, 61.22; H, 4.89; N, 10.81%. ^{1}H NMR (acetone-d^6): See Table 2. ^{13}C NMR (acetone-d^6): δ 157.9 (bpy2), 155.4 (bpy2′), 151.8 (bpy6), 149.6 (bpy6′), 147.2 (Mes1), 141.7 (Mes2), 141.2 (bpy4), 140.4 (bpy4′), 131.2 (Mes4), 128.2 (bpy3), 128.0 (bpy3′), 126.9 (Mes3), 123.0 (bpy5), 119.3 (bpy5′), 112.1 (S*C*N), 24.9 (*o*-CH_3), 20.7 (*p*-CH_3). UV−vis (acetone): 445 nm. IR (film): 2921s, 2098vs ($\nu_{N\equiv C}$ → SCN is S-bonded), 1730m, 1604m, 1442s, 1143m, 1013 m, 852m, 765s, 736s cm^{-1}. The compound was first mentioned in a report by Seidel in 1985,[28] but characterization remained undone.

Results and Discussion

Preparation and Analyses. The complexes [(bpy)Ni-(Mes)X] (X = Cl, Br) were prepared from *trans*-[$(PPh_3)_2$Ni(Mes)X] and bpy as described for X = Br.[12,14] The complexes [(bpy)Ni(Mes)X] (X = F or I) were obtained from [(bpy)Ni(Mes)Br] by a salt metathesis reaction using TlF or NaI, respectively. The complexes with X = OMe or SCN were prepared by abstraction of Br from the bromide complex using $AgSbF_6$ and the addition of the corresponding anion (KSCN or NaOMe). All complexes were obtained as air-stable bright red microcrystalline material in good yields. For long-time storage, the complexes have to be saved from humidity. From elemental analyses and ^{1}H NMR spectroscopy, the entity and high-purity of the obtained materials is evident (details in the Experimental Section). The fluoride coligand reveals a ^{19}F NMR signal at −407 ppm, which is typical for F ligands in square-planar organonickel(II)

(23) (a) Becke, A. D. *J. Chem. Phys.* **1993**, *98*, 5648–5652. (b) Becke, A. D. *Phys. Rev. A* **1988**, *38*, 3098–3100.
(24) (a) Perdew, J. P.; Burke, K.; Ernzerhof, M. *Phys. Rev. Lett.* **1996**, *77*, 3865–3868. (b) Perdew, J. P. *Phys. Rev. A* **1986**, *33*, 8822–8824.
(25) Hariharan, P. C.; Pople, J. A. *Theor. Chim. Acta* **1973**, *28*, 213–222.
(26) Rassolov, V. A.; Pople, J. A.; Ratner, M. A.; Windus, T. L. *J. Chem. Phys.* **1998**, *109*, 1223–1229.
(27) Cossi, M.; Rega, N.; Scalmani, G.; Barone, V. *J. Comput. Chem.* **2003**, *24*, 669–681.
(28) Seidel, W. *Z. Chem.* **1985**, *25*, 411–412.

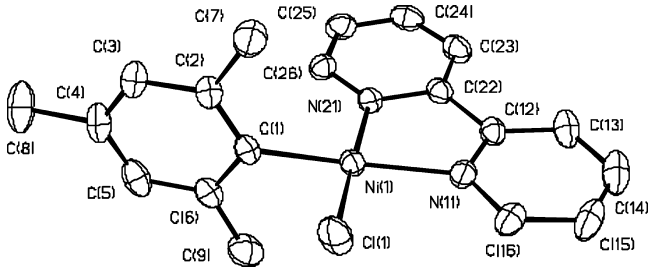

Figure 1. Molecular structure of [(bpy)Ni(Mes)Cl] showing the atomic numbering scheme. The probability ellipsoids are drawn at the 50% probability level. H atoms are omitted for clarity.

complexes.[29,30] The OMe and SCN coligands show characteristic signals for their ^{1}H or ^{13}C atoms. A closer look at the ^{1}H NMR data (Table 2) reveals that the signals of the 6 and 6′ protons are extremely different. The H(6) proton is strongly deshielded by the close-by halide coligand; the H(6′) proton in contrast is strongly shielded by the π system of the aromatic Mes coligand. It is interesting to note that these effects show almost the same magnitude for F, Cl, and Br. The deshielding effect of the I coligand is largest in that series; the pseudohalide ligands OMe and SCN do not exhibit a deshielding effect of the same magnitude.

Crystal Structure of [(bpy)Ni(Mes)X] (X = Cl or I). From concentrated solutions of the complexes [(bpy)Ni(Mes)X] (X = Cl or I) in toluene, we obtained suitable single crystals for X-ray diffraction (XRD). The compounds were found to crystallize in the monoclinic space groups $P2_1/c$ for X = I and $P2_1/n$ for X = Cl (for details, see Table 1). In both crystal structures, no intermolecular contacts were found; for X = I, the unit cell contains two independent molecules.

The molecules show an almost planar coordination sphere around the nickel atom; the mesityl coligand is oriented almost perpendicular to the coordination plane. As an example, Figure 1 displays the molecular structure of [(bpy)Ni(Mes)Cl]; selected structural data is summarized together with data from the X = Br derivative[13] in Table 3.

As expected from the stronger trans influence of the formal carbanionic mesityl coligand compared to the weaker X coligands, the Ni−N(11) bond is markedly longer than Ni−N(21). The observed Ni−X distances are in excellent agreement with the sum of the covalent radii (2.15 Å for Cl, 2.30 Å for Br, and 2.49 Å for I, see Table 4), pointing to polar covalent character of the Ni−X bond. Other variations in bond parameters like, for example, the C(1)−Ni−N(11) angle, which ranges from 170 to 176°, or the interring dihedral angle of the two pyridine units, which shows variations from 5 to 12°, do not indicate a clear trend within the series. The chelate bite angle N−Ni−N seems to be fixed for all systems to about 82°, a value which has also been observed for related systems.[12−14]

We assume that the system is quite flexible in many parameters to compensate for various constraints from crystal packing. At the same time, we can conclude from our study that the effects imposed by the X coligand on the complex geometry are not dramatic.

X-Ray Spectroscopy of [(bpy)Ni(Mes)X]. In the Ni K edge XANES spectra for all complexes (see Figure 2), the typical two pre-edge peaks of square-planar Ni(II) complexes can be observed.[13,31] The prepeak at about 8333 eV can be assigned to a 1s → 3d electron transition, while the second peak, which occurs at about 8338 eV, is due to a 1s → 4p transition with shakedown contributions.[31a−c] Both observations confirm the square-planar geometry around the nickel(II) atom. For comparison, the "edge energies" of the XANES spectra were determined as the energy corresponding to a normalized absorption of 0.5. These edge energies decrease slightly from F (8341.95 eV) to I (8340.77 eV), indicating the highest electron-donating power for the I coligand (see Figure 2, right).

Figure 3 shows the k^3-weighted experimental and fitted EXAFS spectra of the complexes [(bpy)Ni(Mes)X] along with the magnitudes of their Fourier transforms in r space. The obtained structural parameters of the investigated complexes determined by a curve-fitting analysis of the EXAFS spectra are summarized in Table 4.

The fitting of the Ni K edge EXAFS spectra was performed using a three-shell model, in which the first coordination shell at about 1.93 Å comprises the two coordinating nitrogen atoms of the diimine ligand and the carbon atom of the mesityl coligand. The second shell consists of the halogen backscatterer, and the third coordination shell at ∼2.8 Å contains six backbone-carbon atoms of the mesityl and diimine ligand. In the first shell, the nitrogen and carbon backscatterers cannot be distinguished, because of their similar distances and backscattering amplitudes. Therefore, they were fitted as one shell with nitrogen amplitude and phase functions.

The data obtained from EXAFS are in good agreement with the parameters from single-crystal XRD for X = Cl, Br, and I (see Table 4). Only the interatomic distances of the third shells are on average 0.05 Å smaller than the XRD values. There are two main reasons for this larger error: (i) carbon atoms are weak backscatterers with a small signal at a distance of 2.8 Å; (ii) the third shells consist of six different carbon atoms with interatomic distances ranging from 2.77 to 3.01 Å. This distance distribution also gives rise to the relatively high Debye−Waller factors of the third shells. For the F derivative, the same type of fit was used as for the other three complexes. Here, the fluorine and N(bpy)/C(Mes)

(29) (a) Steffen, A.; Sladek, M. I.; Braun, T.; Neumann, B.; Stammler, H.-G. *Organometallics* **2005**, *24*, 4062–4064. (b) Braun, T.; Perutz, R. N. *Chem. Commun.* **2002**, 2749–2757. (c) Braun, T.; Foxon, S. P.; Perutz, R. N.; Walton, P. H. *Angew. Chem., Int. Ed.* **1999**, *38*, 3326–3329.

(30) Burling, S.; Elliott, P. I. P.; Jasim, N. A.; Lindup, R. J.; McKenna, J.; Perutz, R. N.; Archibald, S. J.; Whitwood, A. C. *Dalton Trans.* **2005**, *368*, 6–3695.

(31) (a) Colpas, G. J.; Maroney, M. J.; Bagyinka, C.; Kumar, M.; Willis, W. S.; Suib, S. L.; Baidya, N.; Mascharak, P. K. *Inorg. Chem.* **1991**, *30*, 920–928. (b) Ottenwaelder, X.; Aukauloo, A.; Journaux, Y.; Carrasco, R.; Cano, J.; Cervera, B.; Castro, I.; Curreli, S.; Munoz, M. C.; Rosello, A. L.; Soto, B.; Ruiz-Garcia, R. *Dalton Trans.* **2005**, 2516–2526. (c) DuBois, J. L.; Mukherjee, P.; Stack, T. D. P.; Hedman, B.; Solomon, E. I.; Hodgson, K. O. *J. Am. Chem. Soc.* **2000**, *122*, 5775–5787. (d) Renner, M. W.; Furenlid, L. R.; Barkigia, K. M.; Fajer, J. *J. Phys. IV France* **1997**, *7* (C2), 661–663. (e) Kosugi, N.; Yokoyama, T.; Asakura, K.; Kuroda, H. *Chem. Phys.* **1984**, *91*, 249–256. (f) Kosugi, N.; Yokoyama, T.; Kuroda, H. *Chem. Phys.* **1986**, *104*, 449–453.

Table 3. Selected Bond Lengths (Å) and Angles (deg) of [(bpy)Ni(Mes)X]

	X = Cl	X = Br[13]		X = I	
		molecule 1	molecule 2	molecule 1	molecule 2
		Bond Lengths (Å)			
Ni(1)−X(1)	2.1577(11)	2.2977(12)	2.3024(14)	2.4678(10)	2.4661(10)
Ni(1)−C(1)	1.901(3)	1.904(8)	1.887(8)	1.900(5)	1.914(5)
Ni(1)−N(11)	1.985(2)	1.980(6)	1.987(6)	1.984(4)	1.984(4)
Ni(1)−N(21)	1.911(2)	1.895(6)	1.897(6)	1.926(4)	1.912(4)
N(11)−C(16)	1.339(4)	1.347(10)	1.324(10)	1.329(6)	1.348(7)
N(11)−C(12)	1.345(4)	1.326(9)	1.359(10)	1.355(6)	1.355(7)
N(21)−C(26)	1.341(4)	1.361(10)	1.333(10)	1.349(6)	1.354(6)
N(21)−C(22)	1.365(3)	1.352(10)	1.376(10)	1.357(6)	1.363(6)
C(12)−C(22)	1.469(4)	1.460(11)	1.456(11)	1.477(7)	1.475(7)
		Angles (deg)			
C(1)−Ni(1)−N(21)	92.92(11)	94.3(3)	93.2(3)	92.73(19)	92.96(19)
C(1)−Ni(1)−N(11)	175.40(11)	176.2(3)	170.4(3)	173.00(18)	173.9(2)
N(21)−Ni(1)−N(11)	82.80(10)	82.2(3)	83.0(3)	82.81(17)	82.80(18)
C(1)−Ni(1)−X(1)	89.16(9)	87.5(2)	88.3(2)	86.59(14)	87.56(15)
N(21)−Ni(1)−X(1)	174.91(7)	177.5(2)	172.1(2)	171.56(13)	174.11(13)
N(11)−Ni(1)−X(1)	95.24(8)	96.0(2)	96.8(2)	98.62(12)	97.10(13)
sum of angles around Ni(1)	360.12	360.00	361.30	360.75	360.42
		Dihedral Angles (deg)			
N−M−N/X−Ni−C_{Mes}	5	8.6	12.1	10.2	7.5
Py(1)/Py(2)[a]	2.2	1.9	10.5	5.0	5.4
Py/N,M,N,C(12),C(22)[b]	2.2, 2.5	1.4, 1.8	3.8, 7.1	2.9, 5.0	2.1, 4.1
Mes/C_{Mes},N,M,N,X[c]	90.9	92.9	93.4	90.2	84.7

[a] Py represents the pyridine units of the chelate ligand bpy. [b] N,M,N,C(12),C(22) defines the chelate five ring. [c] C_{Mes},N,M,N,X defines the coordination plane.

Table 4. Structural Parameters of the Solid Complexes [(bpy)Ni(Mes)X] Determined from the Ni K-Edge EXAFS Spectra in Comparison to XRD Data and ADF/BP Calculations

X		r (Å)[a]	N[a]	σ (Å)[a]	E_f (eV)[a]	fit-index[a]	XRD data (Å)	calcd data[b] (Å)
I	Ni−C/N[c]	1.93(2)	3	0.074(7)	8.11	28.47	1.94	1.940
	Ni−I	2.47(2)	1	0.081(8)			2.47	2.505
	Ni···C[d]	2.81[e]	6	0.15(2)			2.88	2.892
Br	Ni−C/N[c]	1.92(2)	3	0.074(7)	7.86	21.50	1.93	1.934
	Ni−Br	2.29(2)	1	0.059(6)			2.30	2.299
	Ni···C[d]	2.82[e]	6	0.10(2)			2.87	2.885
Cl	Ni−C/N[c]	1.93(2)	3	0.089(9)	7.41	33.29	1.93	1.933
	Ni−Cl	2.16(2)	1	0.074(7)			2.16	2.158
	Ni···C[d]	2. 84[e]	6	0.10(2)			2.88	2.889
F	Ni−C/N[c]	2.05[e]	3	0.055[e]	2.89	34.56		1.917
	Ni−F	1.88[e]	1	0.045[e]				1.792
	Ni···C[d]	2.93[e]	6	0.12(2)				2.891

[a] Absorber−backscatterer distance, r; coordination number, N; Debye−Waller factor, σ; edge position, E_f (Fermi energy) relative to calculated vacuum zero; fit-index, R, for a fitted k range from 3.0 to 15.5 Å^{-1}. The numbers in parentheses are uncertainties in the last digit. The errors are estimated to be ±1% for distances, ±10% for Debye−Waller factors of shells with r < 2.5 Å, and ±15% for Debye−Waller factors of shells with r > 2.5 Å. [b] From ADF/BP calculations (see below). [c] N(bpy) and C(Mes) atoms. [d] 4C(bpy) + 2C(Mes) atoms. [e] Errors higher than the estimates given above due to strong correlation between different shells (see text).

backscatterers could be fitted at 1.88 Å and 2.05 Å, respectively. The latter value is significantly different from the first-shell distances of the other complexes (about 1.93 Å). The reason for this discrepancy is that the backscattering amplitudes and interatomic distances of fluorine, carbon, and nitrogen are very similar. Therefore, in the fitting procedure, the N(bpy)/C(Mes) contribution cannot be separated unambiguously from the fluorine signal, which leads to this inaccurate Ni−C/N distance. Accordingly, also the real Ni−F distance might deviate distinctly from the fitted value of 1.88 Å. The third shell consisting of six backbone-carbon atoms could be fitted at 2.93 Å, which is in good agreement with the corresponding XRD values (from single crystals) of the Cl, Br, and I complexes.

The observed Ni−F bond length of 1.88 Å is slightly longer than the sum of the covalent radii of 1.80 Å (see Table 5) and in good agreement with related structurally characterized organometallic complexes like *cis*-[(dippe)Ni(CH_3)F] (dippe = di(isopropylphosphino)ethane), with a Ni−F distance of 1.860(2),[32] or *cis*-[(dchpe)Ni(C_5NF_4)F] (dchpe = di(cyclohexylphosphino)ethane),[30] in which the Ni−F distance lies around 1.85 Å (averaged for two molecules). An examination of Ni−F distances in the Cambridge Structural Database reveals a bimodal distribution of Ni−F distances, with one group showing a mean Ni−F distance of 1.86 Å and a second group revealing a mean distance of 2.03 Å. The latter group is represented by complexes like *trans*-[$(py)_4NiF_2$],[33] with an octahedrally configured nickel atom and two electrons in the e_g antibonding orbital. The first

(32) Cámpora, J.; Matas, I.; Palma, P.; Graiff, C.; Tiripicchio, A. *Organometallics* **2005**, *24*, 2827–2830.
(33) (a) Halasyamani, P.; Willis, M. J.; Stem, C. L.; Poeppelmeier, K. R. *Inorg. Chim. Acta* **1995**, *240*, 109–115. (b) Holzbock, J.; Sawodny, W.; Walz, L. *Z. Kristallogr.* **1997**, *212*, 115–120.

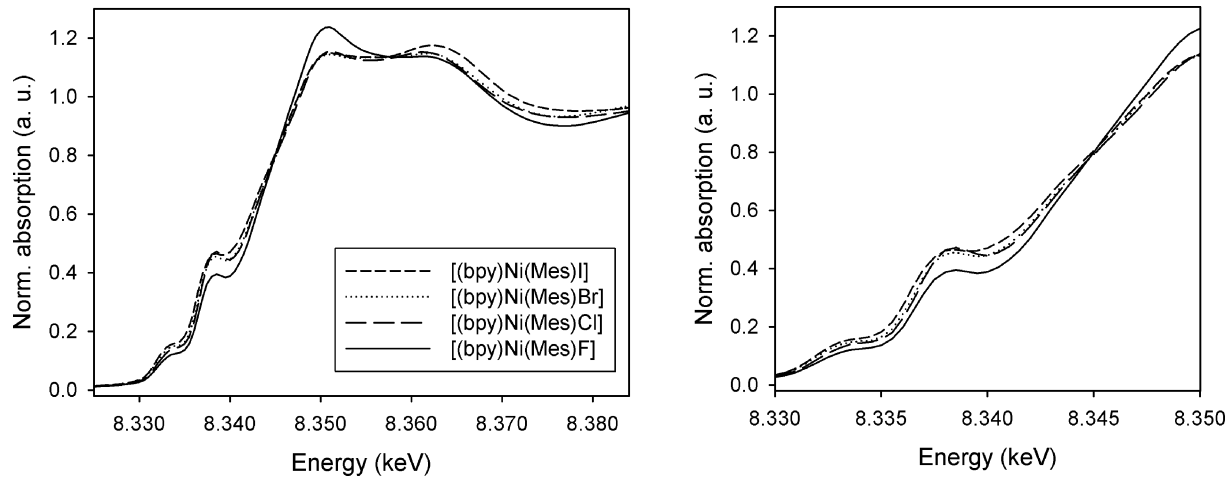

Figure 2. Comparison of the normalized XANES spectra of the solid samples [(bpy)Ni(Mes)X] (with X = F, Cl, Br, I) measured at the Ni K edge. On the right: Magnified edge region of the four complexes.

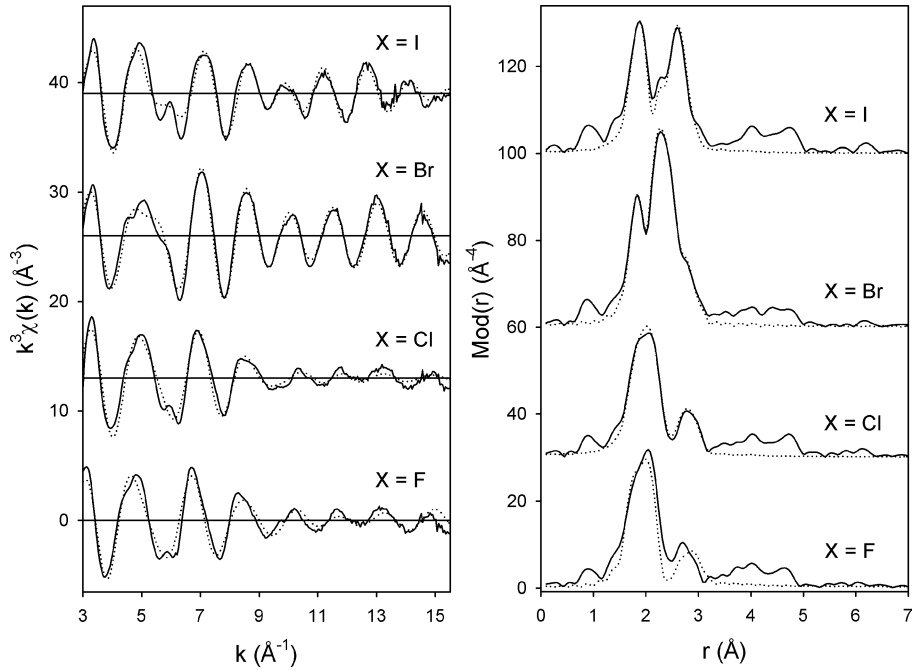

Figure 3. Experimental (solid line) and calculated (dotted line) k^3 $\chi(k)$ EXAFS functions (left) and their Fourier transforms (right) of the solid samples [(bpy)Ni(Mes)X] measured at the Ni K edge. Spectra for X = Cl, Br, and I are shifted on the y axes for clarity.

Table 5. Covalent vs Ionic Radii of Ni and the X Atoms and Observed Ni−X Distances in Complexes [(bpy)Ni(Mes)X]

	Ni	F	Cl	Br	I
r_{cov}/r_{ionic} (Å)	1.16[a]/0.63	0.64/1.36	0.99/1.67	1.14/1.82	1.33/2.06
∑(rNi + X) (Å)		1.80/1.99	2.15/2.30	2.30/2.45	2.49/2.69
rNi−X exp. XRD (Å)			2.1577(11)	2.3000(13)[b]	2.4669(10)[b]
rNi−X exp. EXAFS (Å)		1.88	2.16	2.29	2.47

[a] The covalent radius for Ni is not unequivocal since it is strongly dependent on the oxidation state and ligand surroundings. The value of 1.16 Å has been widely accepted for square-planar Ni(II) complexes;[36] other values are from ref. [b] Averaged values.

group comprises exclusively organometallic nickel complexes with a square-planar configuration. The different electronic situation explains the markedly shortened Ni−F distance in comparison to the nonorganometallic complexes. An intermediate case is met in the binuclear cationic complex $[(\mu\text{-F})\{Ni(bpy)_2F\}_2]^+$ in which the terminal Ni−F bond is longer (2.005(4) Å) than the bridging one (1.985(3) Å).[34] Interestingly, within the group of organometallic complexes, the orientation (*cis* or *trans*) of the F ligand toward the strongly donating organoligand has no marked impact on the Ni−F bond length (in terms of a trans influence).

We can thus conclude that, in organometallic derivatives (including our example), the Ni−F bonds are relatively strong and the degree of covalency seems to be rather high. Both

(34) Emsley, J.; Arif, M.; Bates, P. A.; Hursthouse, M. B. *J. Chem. Soc., Dalton Trans.* **1989**, 1273–1276.

(35) Libri, S.; Jasim, N. A.; Perutz, R. N.; Brammer, L. *J. Am. Chem. Soc.* **2008**, *130*, 7842–7844.

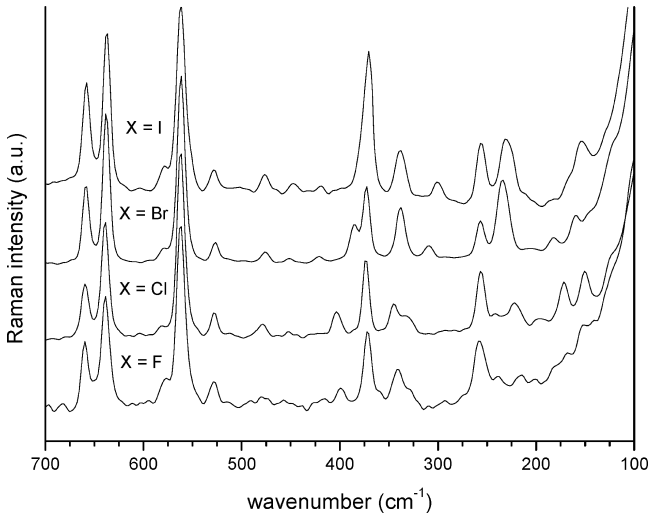

Figure 4. Raman spectra of solid samples of [(bpy)Ni(Mes)X] in the range from 100 to 700 cm^{-1}.

can be explained with the high electron density of the nickel atom in organometallic derivatives fitting well to the high electronegativity of the F atom.

Furthermore, if we compare the Ni−X distances for all four homologous nickel complexes with the calculated sum of the covalent radii (Table 5), only the Ni−F distance slightly exceeds the latter, while for X = Cl, Br, or I, the two fit extremely well. Thus, it seems that all Ni−X bonds in our series are highly covalent, and the (bond prolonging) ionic contribution to the Ni−X bond is highest for fluoride and lowest for X = I. This is in good agreement with a recent report on very strong hydrogen bridging in the system *trans*-$[(C_5F_4N)Ni(PEt_3)_2F\cdots H(indole)]$, indicating a highly polar Ni−F bond in the organonickel complex.[35] In the section on the ligand exchange reaction (see below), we will try to further substantiate the question on the polarity of the Ni−F bond.

Vibrational Spectroscopy (IR and Raman). Assuming the same geometry for the series of isoleptic complexes [(bpy)Ni(Mes)X], we have measured IR and Raman spectra to probe for the influence of the X coligand. A comparison of the spectra reveals only very subtle changes in the spectra going through the series of X coligands, as exemplified in Figure 4 for the Raman spectra in the range 100−700 cm^{-1} (a detailed lists of Raman frequencies in the range from 3200 to 200 cm^{-1} and further spectra can be found in the Supporting Information). Table 6 reveals that DFT calculated Raman active vibrations only slightly depend on ligand X and reasonably describe the experimental spectrum. No resonances from clearly defined vibrations like ν(Ni−X), which were expected in this region, were discernible. The calculations show that M−X stretching modes are strongly coupled to other modes; thus, these bands (at around 400 and 330 cm^{-1}) are almost invariant to the change of X, and they contribute only to rather weak transitions. Also, other Raman active features in this part of the spectrum cannot be assigned to single isolated vibrations; Table 6 indicates the prevailing contribution to individual vibrations.

Absorption Spectroscopy and Quantum Chemical Calculations. The absorption spectrum of [(bpy)Ni(Mes)Br] has been reported and analyzed by quantum chemical calculations recently, together with the spectra of [(bpy)Ni(Mes)$_2$] and [(bpy)Ni(Me)$_2$].[14] The long-wavelength absorption band system for the bromide-containing derivative was found to be blue-shifted compared to the dimesityl and dimethyl complexes; the found negative solvatochromism for the former is largely enhanced, but the overall character does not differ markedly. The quantum chemical calculations revealed contributions of bromine p orbitals to the highest occupied molecular orbitals (HOMOs) up to 42%; resonance Raman investigations however could not establish unequivocally the bromide coligand as a part of the molecules' chromophore. The variation of the X coligand was thus sought in order to support the assignment. However, Figure 5 (data collected in Table 7) reveals that the long-wavelength absorption bands of the complexes do not vary markedly. There is only a slight red shift upon going from X = F to I. The extinction coefficients which have been determined with an accuracy of ±200 $M^{-1}cm^{-1}$ show an increase in the same direction.

Thus, new DFT calculations on the present systems [(bpy)Ni(Mes)X] were carried out using two different program packages: Gaussian 03 and ADF. Both approaches describe the structures of all systems quite well; however, the ADF/BP method yields structural parameters slightly closer to the experimental values. ADF/BP calculated selected bond lengths and angles are compared with experimental ones in Table S11 (Supporting Information).

The composition of the frontier molecular orbitals is almost the same for all four complexes. The closely lying set of HOMOs is formed either by Ni 3d orbitals or π orbitals of the mesityl coligand. The three lowest-lying unoccupied orbitals formed predominantly by π^* bpy orbitals are followed by the antibonding Ni 3d orbital. A full data summary can be found in Tables S12−S15 in the Supporting Information. In contrast to the previous calculations on the [(bpy)Ni(Mes)Br] system,[14] the contribution of the X coligand to the HOMO was found to be marginal for X = F and Cl and is only slightly increasing within the series going from F to I. The reason lies in the different type of calculation applied. The previous work consisted of ADF in vacuo calculations,[14] whereas the present calculations include the solvent effect (G03/B3LYP/CPCM).

Additionally, the corresponding TD DFT (G03/B3LYP/CPCM) calculated transitions reveal that, although the I atom and in part also Br contribute to the HOMOs, their involvement in the electronic transitions is negligible, and the absorption spectra should thus be invariant to the variation of X. Table 7 lists experimental and TD DFT (G03/B3LYP/CPCM) calculated wavelengths. Selected lowest calculated TD DFT excitation energies, together with the composition of individual transitions, are presented in Tables S16−S19 in the Supporting Information. The simulated electronic spectrum of [(bpy)Ni(Mes)Br] depicted in Figure 6 quali-

(36) Kilbourne, B. T.; Powell, H. M. *J. Chem. Soc. (A)* **1970**, 1688–1693.
(37) Shriver, D. F.; Atkins, P. W.; Langford, C. H. *Inorganic Chemistry*, 2nd ed.; Oxford University Press: Oxford, U.K., 1994.

Table 6. Experimental and DFT/B3LYP Calculated Raman Active Bands for [(bpy)Ni(Mes)X] in the Range from 200 to 700 cm^{-1}

X = F		X = Cl		X = Br		X = I		
exptl	calcd[a]	exptl	calcd[a]	exptl	calcd[a]	exptl	calcd[a]	Prevailing vibrations
660	658	659	651	658	651	658	652	νNi−N (sym) + δ (CH)
639	634	638	622	638	622	638	622	νNi−N (antisym) + δ (CH)
562	548	562	555	562	554	562	553	δ (N−Ni−C) + δ (Mes)
	543		551		552		548	δ (N−Ni−C) + δ (Mes)
529	520	527	552	527	552	527	518	δ (Mes)
399	417	405	400	387	389	375	376	δ (Mes) + νNi−X
372	374	373	370	372	369	371	368	δ (N−Ni−N) (sym)
340	367	345	339	338	336	338	335	δ (Mes) + νNi−C
332	351	330	339	310	317	301	299	δ (Mes) + νNi−X
258	253	257	246	256	246	253	244	δ (bpy)
216	226	223	233	236	229	231	223	δ (bpy)

[a] Calculated values were scaled by the factor 0.963.

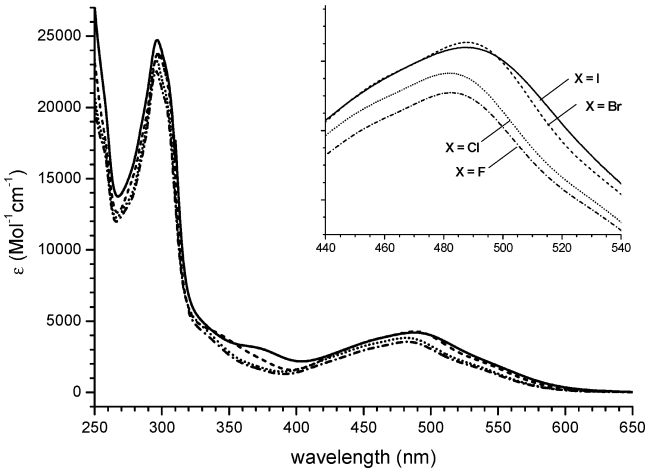

Figure 5. Absorption spectra of [(bpy)Ni(Mes)X] in dichloromethane solution.

Table 7. Experimental Long-Wavelength Absorption Maxima of Complexes [(bpy)Ni(Mes)X] in Dichloromethane Solution Compared with TD DFT (B3LYP/CPCM) Calculated Wavelengths and Oscillator Strengths

		λ (nm), ε (M^{-1} cm^{-1}), or calcd oscillator strength				
(X)		λ_1	λ_2	λ_3	λ_4	λ_5
F	exptl λ	242	295	460sh	482	526sh
	ε	22500	22640	3210	3560	1980
	calcd λ	226	284	425	476, 493	610
	osc. str.	0.318	0.497	0.086	0.009, 0.004	0.008
Cl	exptl λ	244	298	463sh	483	530sh
	ε	24000	23860	3520	3820	2010
	calcd λ	237	285	425	476, 493	600
	osc. str.	0.316	0.528	0.086	0.004, 0.009	0.006
Br	exptl λ	245	297	463sh	489	532sh
	ε	24900	23820	3810	4290	2320
	calcd λ	230	285	429	484	621
	osc. str.	0.460	0.528	0.089	0.012	0.003
I	exptl λ	243	298	467sh	491	532sh
	ε	26800	25100	3910	4210	2540
	calcd λ	237	287	434	493	521, 653
	osc. str.	0.342	0.448	0.091	0.019	0.004, 0.003
OMe	exptl λ	243	284	445sh	464	518sh
	ε	21000	13980	1570	1680	720
SCN	exptl λ	238	289	432sh	452	495
	ε	27700	27100	2900	3000	1700

tatively represents the experimental spectrum of this complex.

The calculated and the experimental absorption data agree qualitatively quite well. The calculation allows good reproduction of the intensity ratio between the UV ($\pi-\pi^*$) bands (λ_1 and λ_2) and the charge transfer bands in the visible region

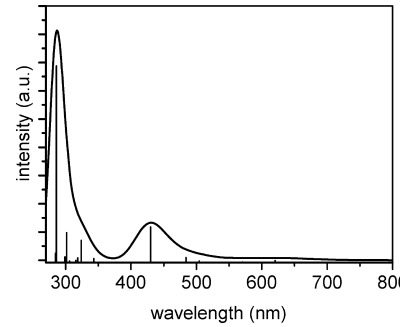

Figure 6. The simulated electronic spectrum of [(bpy)Ni(Mes)Br] based on G03/B3LYP/CPCM (dichloromethane) calculated excitation energies and oscillator strengths (represented by vertical lines).

(λ_{3-5}). The calculation also reveals, in full agreement with the experimental data, that the dominant charge transfer band system in the visible spectrum (λ_3 and λ_4), which is responsible for the color of the compounds, is invariant for the coligand X. They thus confirm the assumptions from the calculations of the composition of the states involved in the lowest electronic transitions, which can overall be described as metal(Ni)-to-ligand(bpy) charge transfer with marked contributions from the mesityl coligand to the HOMO.

On the other hand, the calculated energies fail to match the experimentally observed absorption maxima, although a solvent model was included in the procedure. For example, the calculated very long wavelength transitions around 620 nm were not observed in the experimental spectra and might instead be part of the extended band system around 500 nm. Nevertheless, we were quite confident that qualitatively the calculations show the correct electronic situation of the frontier orbitals and the electronic transitions.

A comparison to the complexes containing the pseudohalides OMe or SCN reveals that the latter also show the characteristic charge transfer band system in the visible region. Compared to the halide complexes, their band systems are markedly blue-shifted (Table 7). This is in agreement with a supposed destabilization of the mainly nickel-centered HOMO by the stronger ligands OMe and SCN. The latter is believed to be S-bonded.

Ligand Exchange Reactions. In a recent paper, we reported the instability of the bromide complex [(bpy)Ni(Mes)Br] in strongly donating solvents like pyridine, nitriles, DMF, or DMSO, with a very fast first reaction (eq 3), cleaving the bromide coligand. This is followed by the

splitting of the chelate ligand (eq 4) and in the case of protic solvents the splitting of the mesityl group.[13]

$$[(bpy)Ni(Mes)X] + Solv \overset{k_1}{\rightleftharpoons} [(bpy)Ni(Mes)(Solv)]^+ + X^- \quad (3)$$

$$[(bpy)Ni(Mes)(Solv)]^+ + 2Solv \overset{k_2}{\rightleftharpoons} [(Solv)_3Ni(Mes)]^+ + bpy \quad (4)$$

The rate constant for the system [(bpy)Ni(Mes)Br] + acetonitrile has been determined to be $k_1 = 0.324(6)$ M^{-1} s^{-1} for eq 3 and $k_2 = 0.0041(3)$ $M^{-1}s^{-1}$ for eq 4.[13] Since the splitting of the X coligand is the initial reaction, it was obligatory to test the same reaction with the complete series of halide coligands.

For all systems the reactions of the complexes dissolved in acetone were monitored by UV−vis spectroscopy. Upon the addition of acetonitrile, a rapid bleaching of the long-wavelength band system at about 460 nm was observed and was found to occur qualitatively in the same way for each system. A monoexponential fit (assuming first-order kinetics) thus allows the determination of k_1. For the iodine derivative, we found a very rapid reaction with $k_1 = 0.176(4)$ M^{-1} s^{-1}; for the F and Cl analogues, the rates are much smaller. For X = F, we found $k_1 = 1.54(6) \times 10^{-4}$ M^{-1} s^{-1}; for X = Cl, we determined $k_1 = 5.18(5) \times 10^{-5}$ M^{-1} s^{-1}. We can conclude that the substitution reaction (3) occurs very probably in an associative manner; the rates go along the series F < Cl < Br < I, which is parallel to their leaving group character in organic substitution reactions.[38] This, in turn, means that there is no indication that the Ni−X bond obtains more ionic character for the electronegative elements Cl or F. This is in excellent agreement with other findings in this work but contrasts with the findings for the system *trans*-[$(C_5F_4N)Ni(PEt_3)_2F\cdots H$(indole)] in which a very strong hydrogen bonding indicates a highly polar Ni−F bond in the organonickel complex.[35] However, the F ligand in this complex is located *trans* to the organo coligand, which might enhance the Ni−F bond polarization, whereas in our system, the more electronegative N donor atom of bpy is located trans to the Ni−F bond.

Electrochemistry. The electrochemistry of the bromide complex [(bpy)Ni(Mes)Br] has been studied in detail recently.[15] From this, we knew that, after the first one-electron reduction (E_1), the complex rapidly cleaves the bromide ligand (eq 5), which renders the first reduction wave irreversible (EC process).

$$[(bpy)Ni(Mes)Br] \overset{E_1 + e^-}{\rightleftharpoons} [(bpy)Ni(Mes)Br]^{\bullet -} \overset{C}{\rightleftharpoons} [(bpy)Ni(Mes)(Solv)]^{\bullet} + Br^- \quad (5)$$

The second reduction (E_2) wave is reversible, and is attributed to the reduction of the solvent complex (Eq. 6).

$$[(bpy)Ni(Mes)(Solv)]^{\bullet} \overset{E_2 + e^-}{\rightleftharpoons} [(bpy)Ni(Mes)(Solv)]^{\bullet -} \quad (6)$$

In order to suppress further chemical reactions which follow the EC process,[15] we performed the measurements at −30 °C (in THF). The cathodic peak potentials determined for E_1 are slightly more negative for X = Cl and F (−1.98 V) than for Br (−1.92 V) or I (−1.95 V); the E_2 process occurs for all complexes at −2.08 V, as expected. The differences in the E_1 values are definitely too small to be discussed; the equal E_2 values confirm our previous assignment.

The oxidation of all halide complexes occurs irreversibly around +0.17 V (in CH_2Cl_2), in full agreement with the calculated HOMO of the complexes, which is composed of nickel or Mes(π) orbitals, but obtains no contribution from X. The OMe complex (+0.71 V) and the SCN analogue (+0.55 V) lie markedly higher, which is in agreement with the results from absorption spectroscopy.

Conclusions

Our studies on the isoleptic organonickel complexes [(bpy)Ni(Mes)X] with X = F, Cl, Br, I, OMe, and SCN have revealed that the halide ligands in these systems exhibit some particular properties. (i) They show a strong deshielding NMR effect in their vicinity; for the pseudohalides, this effect is much weaker. (ii) The Ni−X bond is largely covalent, even for fluoride. The Ni−F bonds in organonickel complexes are rather short and seem to be governed by the high electronegativity of the fluorine atom rather than by the trans influence. (iii) The contribution of the halide coligands to the HOMOs in these complexes (π donation) is generally quite weak and decreases along the series I > Br > Cl > F, which parallels the decreasing overlap integrals assumed from the covalent radii.

Acknowledgment. We thank Dr. Ingo Pantenburg for collecting the crystal data for [(bpy)Ni(Mes)Cl], as well as Dr. Wieland Tyrra and Dr. Harald Scherer (University of Cologne) for NMR measurements. The ANKA Angstroemquelle Karlsruhe is acknowledged for the provision of beamtime, and we would like to thank Dr. Stefan Mangold for assistance using beamline XAS. Financial support is acknowledged from the Academy of Sciences of the Czech Republic (S.Z., Grant KAN100400702), from the Ministry of Education of the Czech Republic (S.Z., Grant OC 139), and from the Deutsche Forschungsgemeinschaft (A.K., Grant KL 1194/5−1).

Supporting Information Available: Further tables with full structural data for the structures of [(bpy)Ni(Mes)Cl] and [(bpy)Ni(Mes)I], tables with the complete results of the quantum chemical calculations, and further figures showing the crystal structures (unit cell) of the two complexes, together with further EXAFS, Raman, and IR spectra. This material is available free of charge via the Internet at http://pubs.acs.org.

IC8007365

(38) Jencks, W. P. *Acc. Chem. Res.* **1980**, *13*, 161–169.